Research on Green Scheduling of Power Battery Electrical Performance Test

He-Xin Li

School of Electronic, Electrical Engineering and Physics
Fujian University of Technology
Fuzhou, 350118, P.R. China
641977230@qq.com

Shi-Hao Huang

School of Electronic, Electrical Engineering and Physics
Fujian University of Technology
Fuzhou, 350118, P.R. China
haoshihuang@fjut.edu.cn

Xin-Jian Cai*

School of Electronic, Electrical Engineering and Physics
Fujian University of Technology
Fuzhou, 350118, P.R. China
cxj2001@fjut.edu.cn

*Corresponding author: Xin-Jian Cai

ABSTRACT. *This paper aims at the problem of poor energy saving of the testing equipment when the testing organization tests the electrical performance of the power battery, and aims to conduct research with the goal of minimizing the power consumption of the testing equipment. An attempt to solve the green scheduling problem for electrical performance testing using standard particle swarm algorithms and replacing traditional schemes. First, according to the actual test requirements, the test task is divided into multiple continuous work units, and the time constraint relationship between related work units is described by the work unit correlation. Combined with the detection process, a scheduling model for the task scheduling problem of electrical performance testing is given. Through a two-layer coding strategy, the mapping relationship between the scheduling scheme and the individual particles in the particle swarm optimization algorithm is successfully established. Finally, two sets of simulation experiments with different scheduling scales are carried out. The simulation results show that the energy saving ratio of the method proposed in this paper is increased by 28.45% and 33.51% compared with the traditional method. The energy saving performance of testing equipment has been significantly improved, realizing green scheduling.*
Keywords: Electrical performance test, Green scheduling, Particle swarm optimization

1. **Introduction.** Lithium batteries have the advantages of high energy density, high power density, low self-discharge rate, and no memory effect [1]. Therefore, lithium batteries are gradually becoming active in daily life. Lithium batteries still need to undergo a series of tests after manufacture. Only through partial random inspection or batch full inspection can it leave the factory. At present, the battery detection system is developing

toward the direction of detection efficiency and energy recycling [2]. However, the battery testing organization found that the energy saving effect of the testing equipment is not good when the battery is tested for electrical performance. This problem not only increases the cost input of testing institutions, but also does not conform to the concept of green development. This problem needs to be solved urgently.

GB/T 31486-2015 "Electrical Performance Requirements and Test Methods for Traction Batteries for Electric Vehicles" specifies the electrical performance requirements, test methods and inspection rules for power lithium battery. The electrical performance test of lithium batteries required by this standard includes charge and discharge performance at different temperatures and charge and discharge performance at different rates, and there are many test contents [3]. The battery detection equipment has the function of energy feedback, and the battery pack in the discharge stage during the test can feed back energy to the battery pack or the power grid in the current charging stage. The current testing organization usually adopts a sequential testing scheme for electrical performance testing. The battery pack to be tested will be inserted into the test channel in turn until all the test items of the battery pack are completed and then switch to the next battery pack. This scheme is called the traditional scheme, and its detection execution diagram is shown in Figure 1.
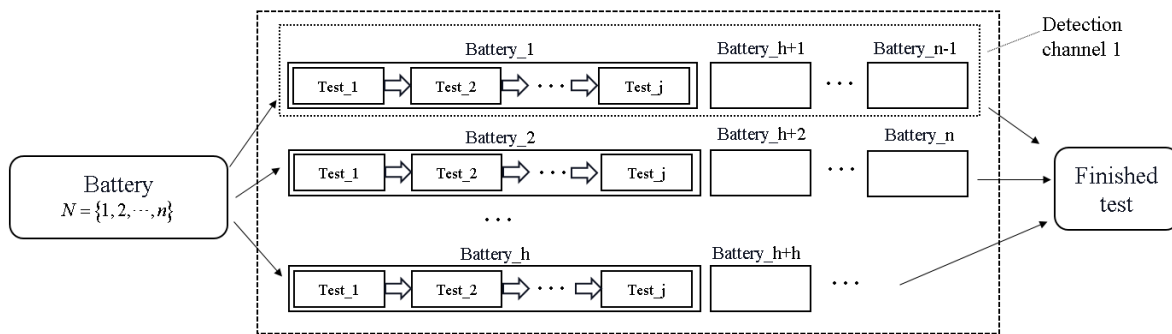
FIGURE 1. Execution diagram of traditional scheme detection

It is not difficult to see that the process flow under the traditional solution is too simple. Traditional solutions do not consider the function of energy feedback between channels. There is little energy feedback process between battery packs, which leads to the problem of poor energy-saving effect of the detection equipment. When the number of battery packs tested in batches increases, the disadvantages of traditional solutions will also be magnified. Therefore, the overall detection efficiency of the detection equipment is low. Testing costs have also increased significantly. Therefore, the current detection process can be studied with green scheduling as the target.

In recent years, more and more scholars have studied green scheduling in the fields of industrial production and manufacturing. Literature [4, 5, 6] considered the energy consumption under different machine states and the energy-saving method of the machine on the basis of the dynamic flexible job shop, and constructs a system based on the minimization of total energy consumption, maximum completion time, total machine load and product quality stability. A high-dimensional multi-objective green dynamic flexible job shop scheduling model for the target, and an improved gray wolf optimization algorithm is designed to solve this problem. Literature [7, 8, 9] aimed at the problem of green sustainable development, through quantitative green index evaluation method, constructs a multi-objective hybrid flow shop scheduling model that minimizes the maximum completion time, carbon emissions and noise, and proposes a hybrid discrete multi-objective

empire competition The algorithm solves the model. Literature [10, 11] comprehensively considered the multi-level organizational structure and task configuration characteristics of the flexible job shop, and proposed a green batch scheduling method for the flexible job shop based on a multi-level optimization model. And based on the difference and interaction relationship of objectives at different scheduling levels, a two-level energy-saving and efficiency-enhancing strategy is developed. Literature [12] developed a model for the flexible job shop scheduling problem, and proposed an energy consumption model to calculate the energy consumption of machines in different states. Then, a non-dominated sorting genetic algorithm is developed to solve the problem. In the non-dominated sorting genetic algorithm, a green scheduling heuristic is proposed to simultaneously optimize manufacturing span, energy consumption, and the number of on/off machines. Literature [13, 14, 15] also aimed at the green scheduling problem, and successfully used the particle swarm optimization algorithm to solve such problems.

In summary, there is no research on the green scheduling problem for battery electrical performance testing. And the scheduling problem has not been solved using intelligent algorithms such as particle swarm algorithm. Since the existing literature has provided systematic analysis and research on the green scheduling problem in other fields, this paper combines the ideas and methods of the above studies in other industrial fields. Therefore, this paper refers to the above mentioned ideas and methods of the existing research in other industrial fields. The article proposes a task scheduling model for electrical performance testing. And the article tries to use the standard particle swarm optimization algorithm. Finally, the scheduling scheme that minimizes the power consumption of the test equipment is successfully solved. The resulting scheduling scheme reduces energy consumption to a certain extent compared with the traditional scheme. Thus, the goal of green testing is realized.

2. **Characteristics of Green Scheduling Problems for Electrical Performance Testing.** Scheduling problem refers to: for a decomposable job, under the premise of certain constraints, in order to achieve the optimization of a certain goal, such as the optimization of total manufacturing time and total manufacturing cost, reasonably arrange the processing time occupied by each component. Time, resources and sequencing [16]. Obviously, the green scheduling problem of electrical performance testing can be studied with reference to the scheduling problem in the industrial field.

Integrating GB/T 31486-2015 and traditional detection schemes, the electrical performance test has the following characteristics: the battery detection channel can perform all electrical performance tests, and the test uses a charge-discharge mode with a fixed rate current, so all charge-discharge processes will have a theory Time, that is, the hourly rate (the time required for the battery to discharge from the rated capacity to the end-of-discharge voltage at a constant current, or the time required for the battery to charge to the rated capacity under the state of the end-of-discharge voltage) [17]. At the same time, task correlation is proposed in the test task scheduling to describe the resource occupation between two tasks [18]. In electrical performance test scheduling, each detection task is divided into several work units, and it is found that there are similar constraints among some work units. For example, some work units cannot proceed to the next work unit immediately after completion, and the battery needs to be put on hold for a period of time before it can enter the next work unit for testing. The time constraint between work units is an occupation relationship for time resources. Therefore, in the following, this constraint is called unit of work dependency.

2.1. **Unit of work dependencies.** Unit of work dependency is used to describe a resource occupancy relationship between two or more work units, and its definition is as follows. This paper defines 1: unit of work dependencies. In addition to the sequence constraints between consecutive work units in the same test, there are certain constraints between the start time and end time of different continuous work units, which are called work unit dependencies. This paper defines 2: related pre-work units and related post-work units. If there is a work unit correlation between two different continuous work units in the same test task, the continuous work unit executed in the front is the relevant pre-work unit, and the continuous work unit executed in the back is the relevant post-work unit.

If there is a correlation between two work units, there are usually the following four forms: the start time of the work unit before the correlation to the start time of the work unit after the correlation, denoted as R_{SS}, the start time of the work unit before the correlation to the end time of the work unit after the correlation, denoted as R_{SF}, the end time of the pre-correlation work unit to the start time of the post-correlation work unit, denoted as R_{FS}, and the end time of the pre-correlation work unit to the end time of the post-correlation work unit, denoted as R_{FF}.

For example, if there is a correlation between two continuous working units O_{ija} and O_{ijb} ($a \neq b, a, b \in k$) in the jth process O_{ij} of the battery pack O_i to be tested, the mathematical expression $R(a, b) = (T_{ab}, t_{ab})$ can be used to express the correlation information between the two, where T_{ab} is the type of correlation ($T_{ab} \in \{R_{SS}, R_{SF}, R_{FS}, R_{FF}\}$), t_{ab} represents the relative time. The start time and end time of work unit O_{ijk} are S_{ijk} and F_{ijk} respectively. There are four kinds of work unit correlations, which can be described algebraically as follows:

If $R(a, b) = (R_{SS}, t_{ab})$, then there is Equation 1.

$$S_{ijb} \geq S_{ijb} + t_{ab} \tag{1}$$

If $R(a, b) = (R_{SF}, t_{ab})$, then there is Equation 2.

$$F_{ijb} \geq S_{ija} + t_{ab} \tag{2}$$

If $R(a, b) = (R_{FS}, t_{ab})$, then there is Equation 3.

$$S_{ijb} \geq F_{ija} + t_{ab} \tag{3}$$

If $R(a, b) = (R_{FF}, t_{ab})$, then there is Equation 4.

$$F_{ijb} \geq F_{ija} + t_{ab} \tag{4}$$

2.2. **Energy conversion mode analysis.** Since the current equipment already has the energy feedback function, it was found during the test that there are many modes of energy flow between the test equipment and the test battery. However, these modes have an important impact on solving the relationship between energies.

Under the condition that the model of the battery pack to be tested is determined, the energy expression provided by a single battery pack can be expressed by Equation 5 [19].

$$E_{BAT} = Q_{BAT} \times U_{BAT} \tag{5}$$

The time for the battery pack to fully discharge can be calculated from the discharge current, as shown in Equation 6.

$$t_{OUT} = Q_{BAT} \div (\eta \times C) \tag{6}$$

For the discharge process of multiple battery packs, it is known that a single battery pack is discharged at a current of ηC, the discharge time is t_{OUT}, and the energy of the battery is:

$$E_{BAT\_OUT} = \sum U_{BAT} \times \eta \times C \times t_{OUT} \qquad (7)$$

For the charging process of multiple battery packs, it is known that a single battery pack is charged at a current of ηC, and the capacity of a single battery pack with a charging time of t_{IN} is Q_{BAT_IN}.

$$Q_{BAT\_IN} = \eta \times C \times t_{IN} \qquad (8)$$

The equivalent total energy is:

$$E_{BAT\_IN} = \sum \frac{Q_{BAT\_IN}}{Q_{BAT}} \times E_{BAT} \qquad (9)$$

(1) Grid side energy supply mode.

This mode is relatively common, that is, in the current time detection sequence, all the energy required by the current battery pack is supplied by the grid side. The energy flow diagram is shown in Figure 2. The energy relationship in this mode is represented by Equation 10.

$$E_{NET\_OUT} = E_{BAT\_IN} \div \eta_{CE} \qquad (10)$$
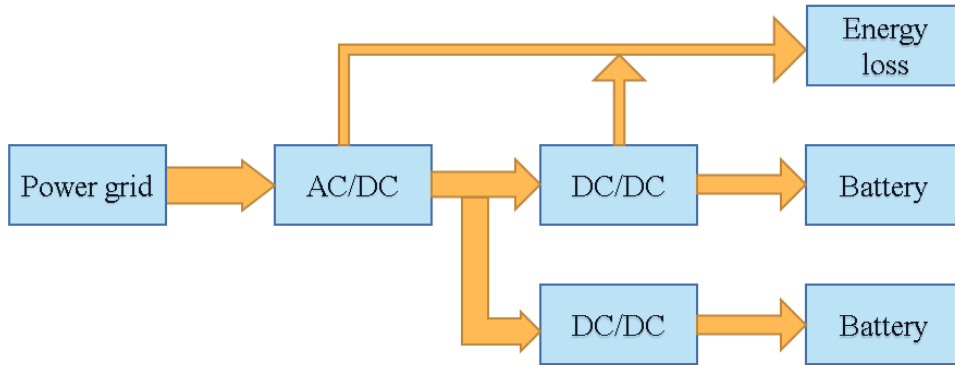
FIGURE 2. Grid side energy supply mod

(2) Battery pack energy supply mode.

On the side of the battery pack, in the current test sequence, the battery pack in the discharge process and the charging process both exist, and the energy released is greater than the energy charged by the battery pack, then the discharged battery pack supplies all the energy of the rechargeable battery pack, and the excess energy is fed back to the grid side. At this time, the energy released by the battery pack will pass through two DC/DC modules when charging each battery pack that needs to be charged. The energy conversion is: the energy of the discharged battery pack is equal to the total energy of the charged battery pack plus the energy fed back to the grid plus the energy lost. The flow diagram is shown in Figure 3. The energy relationship is expressed by Equation 11, and the energy input by the grid side is expressed by Equation 12.

$$E_{BAT\_OUT} = E_{BAT\_IN} \div (\eta_{FE1})^2 + E_{NET\_IN} \div \eta_{FE2} \qquad (11)$$

$$E_{NET\_IN} = \eta_{FE2} \times (E_{BAT\_OUT} - E_{BAT\_IN} \div (\eta_{FE1})^2) \qquad (12)$$
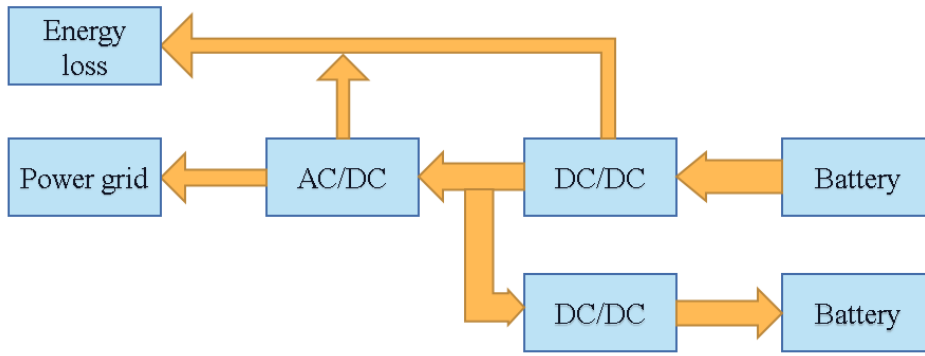
FIGURE 3. Battery pack energy supply mode

(3) Mixed energy supply mode.

In this mode, the same as mode 2, there are also battery packs in the charging phase and discharging phase, but at this time the energy released by the battery pack is not enough to supply energy to the rechargeable battery pack, so energy needs to be supplemented from the grid side. In this mode, the energy is transformed into: charging battery pack energy = discharging battery pack energy + grid supplementary energy - loss energy. The flow diagram is shown in Figure 4. The energy consumed by the grid side is represented by Equation 13.

$$E_{NET\_OUT} = \left(E_{BAT\_IN} - E_{BAT\_OUT} \times (\eta_{FE1})^2\right) \div \eta_{CE} \tag{13}$$
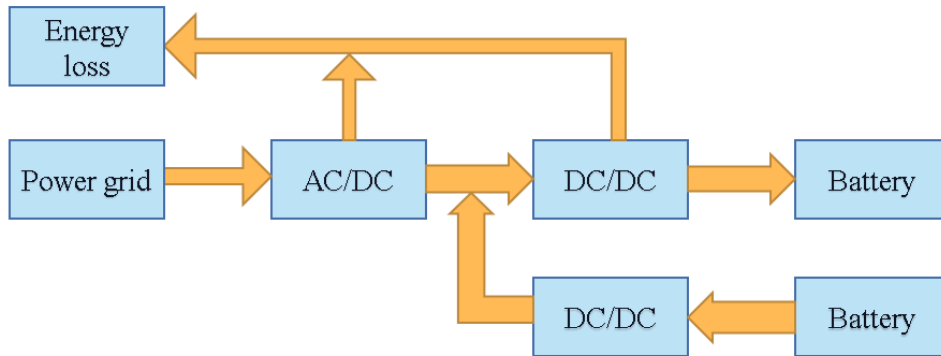
FIGURE 4. Mixed energy supply mode

(4) Electric energy feedback grid mode.

This mode corresponds to mode 1. At this time, the battery pack side is in the discharge stage, and the battery pack needs to release all energy to the grid side. The energy conversion in this mode is: the grid side energy is equal to the total energy of all battery packs minus the loss energy. The flow diagram is shown in Figure 5. The grid side inflow energy is shown in Equation 14.

$$E_{NET\_IN} = E_{BAT\_OUT} \times \eta_{FE2} \tag{14}$$

(5) Battery-battery powered mode.

This mode can be regarded as a special mode of mode 2 and mode 3, and the conditions for its occurrence are relatively harsh. At this time, the energy provided by the battery pack in the discharge phase is just converted into the energy required by the battery pack
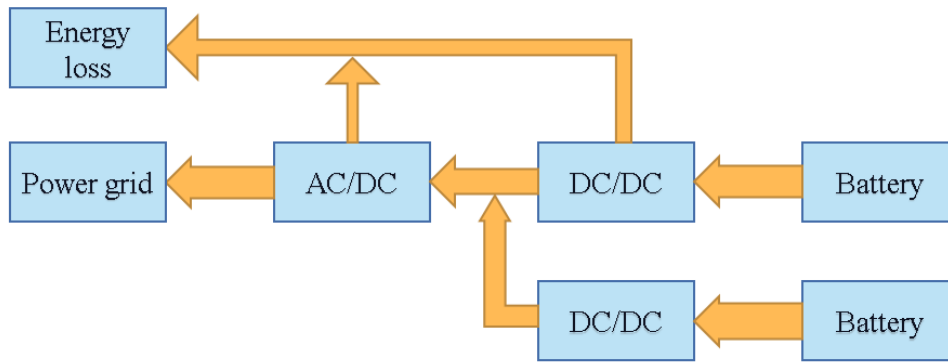
FIGURE 5. Electric energy feedback grid mode

in the charging phase, and the AC/DC module is in the off state, that is, the energy flowing into or out of the grid side is exactly 0. The flow diagram is shown in Figure 6. At the same time, this mode represents an ideal mode, which means that electrical energy can be fully recycled within the system.
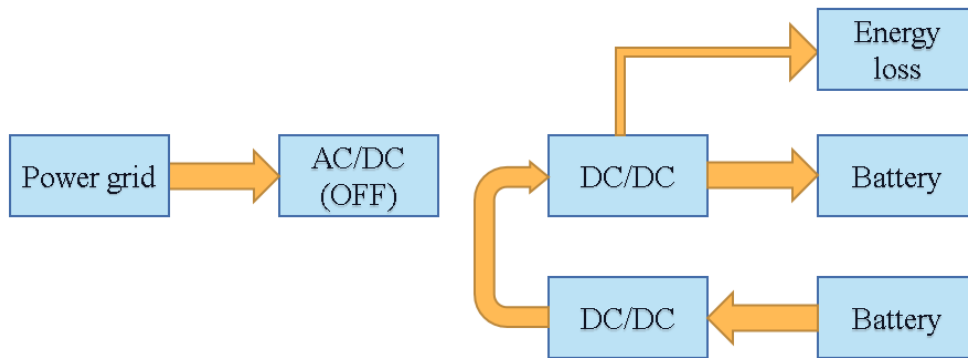
FIGURE 6. Battery-battery powered mode

$$E_{BAT\_IN} = E_{BAT\_OUT} \times (\eta_{FE1})^2 \tag{15}$$

Equation 15 describes the relationship between the energy of the battery pack in the discharge phase and the energy of the battery pack in the charge phase in this mode. It is not difficult to see that when the total energy value of the battery pack exceeds this critical value during the discharge phase, and the excess energy of the discharged battery pack needs to be fed back to the grid side, the energy supply mode will change to the battery pack power supply mode, that is, mode 2; similarly, when When the total energy value of the battery pack in the discharge phase is lower than this critical value, the battery pack in the charging phase has not reached the charging termination state, and the grid side needs to provide the remaining required energy, and the energy supply mode will change to a hybrid energy supply mode. That is mode 3. Therefore, the battery-battery power supply mode can be regarded as the critical mode between the battery pack power supply mode and the hybrid power supply mode, and it is also a condition for judging mode 2 and mode 3. And this mode is an ideal state, that is, the energy in the equipment is completely recovered, reducing the inflow of energy from the grid side.

2.3. **Build a scheduling model.** There are n battery packs to be tested, and each battery pack O_i needs to perform m electrical performance test tasks, and each test item O_{ij} contains q continuous working units. The test equipment has r detection ports with the same function for battery pack selection. The order of the electrical performance test tasks required by the battery pack O_{ij} is fixed, and the time required for the continuous working unit O_{ij} in each test task O_{ijk} can be obtained from the "Electrical Performance Requirements and Test Methods for Traction Battery for Electric Vehicles", and recorded for P_{ijk}. The time for the battery pack O_i to complete all test tasks is recorded as C_i. $C_{\max}$ is the maximum test completion time. The maximum test completion time is the time when all tasks are completed. And there is a maximum test delivery period of C_{dp}, which requires that $C_{\max}$ cannot exceed C_{dp}. The information of the battery pack to be tested is known. The flow of energy in the test will cause loss. At the same time, the energy conversion efficiency η_{CE} of the test equipment, the efficiency η_{FE1} of the energy feedback in DC/DC module and the efficiency η_{FE2} of the energy feedback grid are known. Through the reasonable scheduling of the test units, the power consumption of the test equipment is the lowest in the entire test process, and the following assumptions are made:

(1) All battery packs to be tested can be tested from zero time.

(2) The preparation work required for the battery pack in the test phase and the time taken to switch the battery pack in the detection channel are negligible.

(3) The battery pack is in an empty state by default, that is, the battery pack needs to undergo the standard charging process provided by the national standard during the test process.

(4) The failure of the testing equipment or the interruption of the test task process due to external factors (such as power failure) are not considered for the time being.

(5) The testing process of all battery packs to be tested is fixed, and the continuous working unit and lay-up time in each task are carried out in accordance with the standard.

(6) Even if the battery packs to be tested are of the same model, the capacity may be slightly different due to differences in materials or other factors, so the calculations are based on their rated values.

(7) The energy of the battery pack to be tested is calculated by Equation 5.

(8) Changes in battery capacity due to temperature changes or other conditions are not considered.

(9) All test tasks can be carried out in any detection channel.

The symbolic parameters involved in the mathematical model are shown in Table 1.

Set the scheduling goal as the solution to the lowest power consumption of the test equipment, that is, the total energy consumption on the grid side is the smallest, then the objective function is shown in Equation 16:

$$f = \min\left(E_{LOSS}\right) \tag{16}$$

The total output energy of the grid side is represented by E_{LOSS}, and Equation 17 further explains the composition of the total output energy of the grid side, that is, the grid side The difference between output energy and input energy.

$$E_{LOSS} = \sum E_{NET\_OUT} - \sum E_{NET\_IN} \tag{17}$$

During the whole test process, there are also the following constraints:

$$F_{ijk}^r = S_{ijk}^r + x_{ijk}^r P_{ijk}^r, \forall i \in N, j \in M, k \in Q, r \in H \tag{18}$$

$$F_{ijk}^r \leq S_{ij(k+1)}^r, \forall i \in N, j \in M, k \in Q, r \in H \tag{19}$$

$$F_{ijk}^r \leq S_{i(j+1)k}^r, \forall i \in N, j \in M, k \in Q, r \in H \tag{20}$$

Table 1. Model parameters table

Symbol	Description
n	The number of battery packs to be tested.
N	The battery pack index set to be tested. $N = \{1, 2, \cdots, n\}$
i	Battery index. $i \in N$
m	Number of test tasks.
M	Test task index collection. $M = \{1, 2, \cdots, m\}$
j	Test task index. $j \in M$
q	The number of continuous work units in a task.
Q	Index collection of consecutive units of work within a task. $Q = \{1, 2, \cdots, q\}$
k	Test task unit index. $k \in Q$
d	Number of detection channels.
H	Detection channel index set. $H = \{1, 2, \cdots, d\}$
r	Detection port index. $r \in H$
O_i	The ith battery pack. $O_i \in \{O_1, O_2, \cdots, O_n\}$
O_{ij}	The jth test task of the ith battery pack. $O_{ij} \in \{O_{i1}, O_{i2}, \cdots, O_{im}\}$
O_{ijk}	The kth continuous working unit of the jth test task of the ith battery pack. $O_{ijk} \in \{O_{ij1}, O_{ij2}, \cdots, O_{ijq}\}$
O_{ijk}^r	The kth continuous working unit of the jth test task of the ith battery pack is detected in the rth detection channel.
P_{ijk}^r	The start time of the unit of work O_{ijk}^r.
S_{ijk}^r	The start time of the unit of work O_{ijk}^r.
F_{ijk}^r	The end time of the unit of work O_{ijk}^r.
T_{ijk}^r	The detection time course interval of the unit of work O_{ijk}^r. $T_{ijk}^r = [S_{ijk}, F_{ijk}]$
Y_{IN}	Set of working cells in charging stages of battery pack.
Y_{OUT}	Set of working cells in battery pack discharge phase.
w_{ijk}	The shelving time that the unit of work O_{ijk} needs before executing the test task.
W_{ijk}	The actual shelving time that the unit of work O_{ijk} elapsed before executing the test task.
x_{ijk}^r	State variables. When $x_{ijk}^r = 1$, it means that O_{ijk} is detecting at the detection channel r, and in other cases $x_{ijk}^r = 0$.
C_i	Battery pack i completes all test task time.
$C_{\max}$	Maximum test completion time, which is the time when the last test of all batteries was completed.
C_{dp}	The maximum delivery period.
E_{NET_IN}	Energy input to the grid side.
E_{NET_OUT}	Energy output from the grid side.
E_{BAT_IN}	Energy input to the battery pack.
E_{BAT_OUT}	The energy output by the battery pack.
E_{LOSS}	The total output energy of the grid side.
E_{BAT}	The total energy produced by the battery pack.
Q_{BAT}	The rated capacity of the battery pack.
U_{BAT}	The rated voltage of the battery pack.
η_{CE}	Detect the power conversion efficiency of the equipment.
η_{FE1}	Power feedback DC/DC module efficiency.
η_{FE2}	Electric energy feedback grid efficiency.

$$\exists O_{ija}, O_{ijb} \in O_{ijk}, R(a,b) = (R_{FS}, t_{ab}), \forall i \in N, j \in M, b \in Q \tag{21}$$

$$t_{ab} = w_{ijb}, \forall i \in N, j \in M, b \in Q \tag{22}$$

$$S_{ijk}^r \geq 0, \forall i \in N, j \in M, k \in Q, r \in H \tag{23}$$

$$\sum_{r=1}^{d} x_{ijk}^r = 1, d \in H \tag{24}$$

$$C_i \geq \max\left(\sum_{j=1}^{m} \sum_{k=1}^{q} \sum_{r=1}^{d} x_{ijk}^r F_{ijk}^r\right) \tag{25}$$

$$C_{max} \geq \max C_i \tag{26}$$

$$C_{dp} \geq C_{max} \tag{27}$$

Among them, Equation 18 indicates that in the testing process, once a test task starts, it must not be interrupted in the middle. Equation 19 indicates that there is a work sequence constraint in the continuous work unit in the test task, that is, the work unit with a smaller value is executed earlier Equation 20 indicates that there is a sequence constraint among the test tasks, that is, the battery needs to complete the previous test task before entering the next test task. Equation 21 indicates that there is a correlation between the working units in the same task. Equation 22 gives the quantitative relationship between the correlation time and the lay-by time. Equation 23 indicates that all battery modules to be tested can be tested at zero time. Equation 24 indicates that all working units can only be tested in one detection channel Equation 25 gives the completion time when all testing items of each battery pack are completed. Equation 26 indicates the completion time of the batch of testing tasks, which is the maximum completion time among all battery packs. Equation 27 indicates that the total test time must not exceed the maximum test delivery period.

3. **Algorithm Design and Implementation.** In recent years, more and more scholars have proposed and used intelligent algorithms to solve various kinds of problems. There are many kinds of intelligent algorithms. The classical algorithms include genetic algorithm, particle swarm algorithm, bee colony algorithm and so on. Many scholars use these algorithms to solve all kinds of problems. And more and more new algorithms have been proposed, such as chaotic-based tumbleweed optimization algorithm (CPPE) [20], phasmatodea population evolution algorithm with chaotic maps CTOA [21] and so on. Benefiting from the rapid development of intelligent algorithms, better results have been achieved for solving certain existing scheduling problems.

PSO was proposed by James Kennedy and Russell Eberhart in 1995 [22]. Its core idea is to find an optimal position information for each particle in the search space, and find a global optimal position from these individuals. The solution is compared with the historical optimal solution, and the best one is selected as the current historical optimal solution. Therefore, each particle has two attributes of position and velocity, and in the optimization process, the particle's own position and velocity information is adjusted through the current individual optimal solution found by the particle and the current global optimal solution of the group. The update speed and position of particles are according to Equation 28 and Equation 29.

$$v_{k+1}^i = w v_k^i + c_1 r_1 \left(p_{best}^i - x_k^i\right) + c_2 r_2 \left(g_{best} - x_k^i\right) \tag{28}$$

$$x_{k+1}^i = x_k^i + v_{k+1}^i \tag{29}$$

In the formula: the position and velocity of the particle in the current round and the next round are respectively determined by x_k^i, v_k^i, x_{k+1}^i And v_{k+1}^i said. w is the inertia weight. c_1 and c_2 represent learning factors. r_1 and r_2 are random values in the

range of $[0, 1]$. p_{best}^i represents the best individual position of particle i in history, and the corresponding best position of global particle history is represented by g_{best}. The individual optimal position and the global optimal position are updated continuously through iterations.

In Eq 28, the velocity v_{k+1}^i of the next round is updated based on the current round velocity v_k^i. This represents the particle's trust in the current state of motion. v_{k+1}^i is the momentum necessary for the particle to make a motion displacement and allows the particle to make inertial motion based on its own velocity. $c_1 r_1 \left(p_{best}^i - x_k^i \right)$ represents the particle's own flight experience. This term represents the particle's "self-awareness" and encourages the particle to fly to the best position it has ever found. $c_1 r_1 \left(p_{best}^i - x_k^i \right)$ represents the current particle's flight experience from other particles, and represents the cooperation and sharing of information between particles. This term describes the "social cognition" of the particles and guides them to the best position in the swarm.

3.1. **Encoding and decoding.** Since PSO is directly aimed at the individual particles, the optimal particle is finally obtained, and the scheduling problem needs to determine the scheduling scheme. The encoding and decoding operations are to establish a mapping relationship between the specific scheduling scheme and the individual population , the operation of converting a scheduling scheme into a particle in the population is called encoding, and the corresponding decoding operation is to convert a particle into a scheduling scheme [23]. Encoding and decoding operations are therefore an important part of linking the optimization algorithm with the actual scheduling problem.

This paper adopts a double-layer coding method. The first layer of coding represents the generated work unit information, and the second layer of coding represents the detection channel information corresponding to the work unit. Since the solution of the electrical performance test scheduling problem is a discrete scheduling sequence, it belongs to a discrete problem. The standard particle swarm optimization algorithm is more suitable for solving continuous variable optimization problems. Therefore, a position-vector-based encoding is used to generate the first layer of encoding. Directly generate position vectors, embedding single-point positions into the search space. Therefore, the generated position points can directly represent the position information of the particles in the particle swarm. The specific operation steps of encoding are as follows:

Step1: First generate an initial code string. The initial code string is related to the scale of the scheduling problem. In the scheduling of electrical performance test tasks, the battery index value is generated. According to the number of battery packs, the index value is generated according to the rule from small to large. The number of index values generated is each battery pack. total number of units of work.

Step2: Establishes a random position range generation interval.

Step3: Randomly generate non-repeating position vector values, and the number of generated values is the same as the length of the initial encoding string.

Step4: The position vector values correspond to the initial encoding. Encoding is complete.

For example, for a scheduling problem with a scheduling scale of 3×4, usually the initial code string is set to 111122223333, and then randomly generate different coordinate values (3.42, 1.78, 0.24, 0.02, 0.45, 1.57, 1.66, 1.78, 2.42 , 3.42, 3.78, 4.67), the coordinate value is the position information of individual particles. Sorting operation is performed on the randomly generated position vectors to obtain a sequence of encoded strings, and the corresponding scheduling scheme can be obtained through decoding. The process is shown in Figure 7.

Generate initial code	1	1	1	1	2	2	2	2	3	3	3	3

Randomly generate position vectors	3.42	1.78	0.24	0.02	0.45	1.57	1.66	3.78	0.22	0.14	4.67	2.42

Sorting operation (Decoding)

Sorted position vector	0.02	0.14	0.22	0.24	0.45	1.57	1.66	1.78	2.42	3.42	3.78	4.67

Generate the sorted encoding	1	3	3	1	2	2	2	1	3	1	2	3

Decode	O_{111}	O_{311}	O_{312}	O_{112}	O_{211}	O_{212}	O_{221}	O_{121}	O_{321}	O_{122}	O_{222}	O_{322}
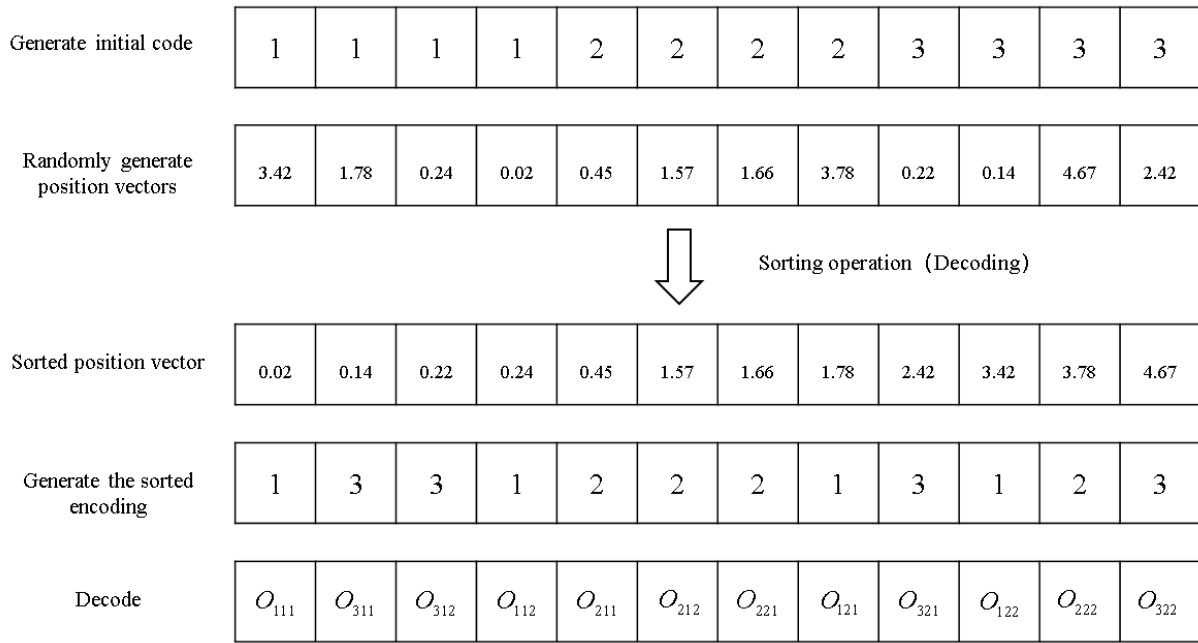
FIGURE 7. Schematic diagram of the first layer of coding

The second layer of coding adopts a kind of coding for random number processing, and the specific operation steps are as follows:

Step1: Randomly generate values within the range.

Step2: Perform absolute value operation on the generated value.

Step3: Divide the obtained value by the total number of detection channels and take the remainder.

Step4: Round up the obtained remainder, and the obtained number is the detection channel information.

For example, the code string of the second layer is randomly generated as (3.23, 1.06, 4.15, 2.64, 1.82, 3.46, 5.23, 3.76, 2.53, 3.11, 0.29, 1.18), and the detection channel code is 221122221212 after decoding. The final corresponding decoding information is (O_{111}^2, O_{311}^2, O_{312}^1, O_{112}^1 , O_{211}^2, O_{212}^2, O_{221}^2, O_{121}^1, O_{321}^1, O_{122}^2, O_{222}^1, O_{322}^2). The above-mentioned second-layer encoding process can be shown in Figure 8.

Randomly generated value	3.23	1.06	4.15	2.64	1.82	3.46	5.23	3.76	2.53	3.11	0.29	1.18

Divide by the number of test channels and take the remainder	1.23	1.06	0.15	0.64	1.82	1.46	1.23	1.76	0.53	1.11	0.29	1.18

Rounded up	2	2	1	1	2	2	2	2	1	2	1	2
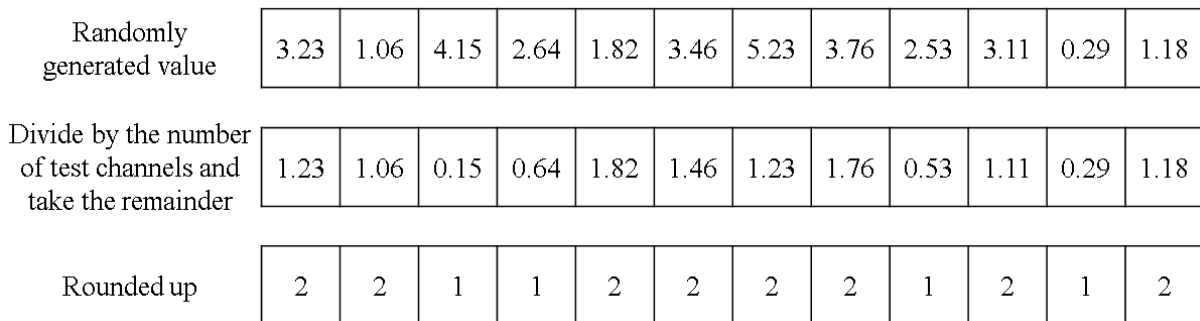
FIGURE 8. Schematic diagram of the second layer coding

After combining the two layers of encoding, the generated scheduling information can be obtained, as shown in Figure 9.

First layer coding	O_{111}	O_{311}	O_{312}	O_{112}	O_{211}	O_{212}	O_{221}	O_{121}	O_{321}	O_{122}	O_{222}	O_{322}
Second layer coding	2	2	1	1	2	2	2	2	1	2	1	2
Encoding information	O^2_{111}	O^2_{311}	O^1_{312}	O^1_{112}	O^2_{211}	O^2_{212}	O^2_{221}	O^2_{121}	O^1_{321}	O^2_{122}	O^1_{222}	O^2_{322}

FIGURE 9. Schematic diagram of double-layer coding

3.2. **Start time calculation.** The currently obtained decoding string only represents the order of work units on all detection channels. Further operations are required to determine the start test time information of each work unit, so as to calculate the energy consumption value generated by the currently generated scheduling scheme.

For any work unit O^r_{ijk}, there is an early detection time interval, that is $\left[\min\left(S^r_{ijk}\right), \infty\right)$. The earliest test start time of this work unit is subject to the following two constraints:

(1) The first constraint is the completion time of the previous working unit of battery pack i, and the previous working unit is O_{iab}. At this time, the detection time range of $[F_{iab} + t_{abjk}, \infty)$. Among them, t_{abjk} is the relative time (if the two work units do not have correlation, it is equivalent to the relative time being 0).

(2) The second constraint is the completion time of the previous work unit of the current detection channel, denoted as $O_{i'j'k'}$. At this time, the detection time range of O_{ijk} is $[F_{i'j'k'}, \infty)$.

Therefore, according to the above two constraints, O_{ijk} can start working time interval as Equation 30. And Equation 30 also represents the testable time interval of the battery pack to be tested for each detection channel at present.

$$\left[\min\left(S^r_{ijk}\right), \infty\right) = [F_{iab} + t_{abjk}, \infty) \bigcap [F_{i'j'k'}, \infty) \tag{30}$$

Due to the properties of the equipment, the efficiency of energy conversion between DC/DC modules is higher than the efficiency of energy fed back to the grid. Therefore, at the current moment, the work arrangement rule of each test channel is to set the discharging process and the charging process of the battery pack that can be arranged to be tested at the same moment. That is, the intersection of the start test time intervals of the work units to be scheduled in each test channel is Equation 31. And the current moment belongs to the test time interval in each test channel.

$$[S, \infty) = [S^r_{ijk}, \infty) \bigcap \cdots \bigcap [S^{r'}_{i'j'k'}, \infty) \tag{31}$$

From this, two time calculation rules can be obtained and summarized as follows:

Calculation rule 1: For the current work unit that needs to be arranged, according to its charge and discharge properties, arrange the work units in the charging phase and the discharging phase at the same time, and the calculation formula is shown in Equation 31.

Calculation rule 2: If the working units that can be arranged to be detected in each detection channel are all in the charging stage or all in the discharging stage. Then the judgment condition in Calculation Rule 1 is invalid, and it is only necessary to arrange the start detection time of the battery pack according to the requirements of Equation 30.

3.3. **Algorithm process.** The process steps of PSO to solve the scheduling problem are as follows:

Step1: Initialize the operation. The number of particle swarms is set to 60.The number of iterations is 250. Learning factors c_1 and c_2 are 2. Inertia weighting of 0.9. The velocity interval is $[0, 10]$. The fitness function is Equation 16.

Step2: Generate initial population.

Step3: Calculate the fitness value of each individual particle in the population according to the fitness function, retain the optimal position of each particle, and retain the best fitness value of the individual and the optimal position of the group so far.

Step4: According to the speed and position update formula, update the particle speed and position.

Step5: Calculate the fitness value of the newly generated particles, and compare the fitness value of the optimal position of each particle with the fitness value of the historical optimal position, if better, replace the historical optimal position with the current the position of the particle.

Step6: For each particle, compare the fitness value of its optimal position with the optimal fitness value of the group, and if it is better, update the optimal position and optimal fitness value of the group.

Step7: Determine whether the current result satisfies the stop condition, or reaches the maximum number of iterations. If so, stop outputting the result. If not, jump to Step3 and continue running until the termination condition is met.

The overall flowchart of the algorithm is shown in Figure 10.

FIGURE 10. Algorithm flowchart

4. **Simulation.** In order to verify the feasibility of the above method, the following simulation experiment is now done. First, the electrical performance test tasks of the battery pack to be tested are: room temperature discharge performance test, room temperature rate discharge performance test, room temperature rate charge performance test, low temperature discharge capacity test and high temperature discharge capacity test. The specific information of each test task is shown in Table 2. Secondly, the set of working unit dependencies within the task of the battery pack to be tested is $\{R(O_{i11}, O_{i12}), R(O_{i13}, O_{i14}), R(O_{i15}, O_{i16}), R(O_{i21}, O_{i22}), R(O_{i31}, O_{i32}), R(O_{i32}, O_{i33}), R(O_{i41}, O_{i42}), R(O_{i51}, O_{i52})\}$. The working unit set of the charging process and the working unit set of the discharging process are shown in Equation 32 and Equation 33.

$$Y_{IN} = \{O_{i11}, O_{i13}, O_{i15}, O_{i21}, O_{i32}, O_{i41}, O_{i51}\} \tag{32}$$

$$Y_{OUT} = \{O_{i12}, O_{i14}, O_{i16}, O_{i22}, O_{i31}, O_{i33}, O_{i42}, O_{i52}\} \tag{33}$$

TABLE 2. Electrical performance test information

Task number	Name	Test time/min	Wait time/min	Number of continuous working units
1	Discharge performance test at room temperature (3 times)	360	180	6
2	Rate discharge performance test at room temperature	80	60	2
3	Room temperature rate charging performance test	90	120	3
4	Low temperature discharge capacity test	120	1500	2
5	High temperature discharge capacity test	120	300	2

4.1. **5×15×2 scheduling scale energy consumption simulation experiment.** In this experiment, the number of battery packs to be tested in this batch is 5, the total number of test working units for each battery pack is 15, and the number of detection channels is 2. The test scale can be expressed as 5×15×2 scheduling scale. The information of the battery pack to be tested is obtained from the test batch information of a certain company. The rated voltage of the battery pack is 25.6V and the rated capacity is 100Ah. The maximum delivery period is 168h. The conversion efficiency of J company's test equipment is 93%, the efficiency of the feedback DC/DC module is 97%, and the efficiency of the feedback grid is 90%. The results of ten runs are taken, and the energy consumption results are kept to two decimal places. The data are shown in Table 3.

Table 3 shows the optimized value obtained by running the algorithm for 10 times. The minimum dispatched value calculated in Experiment 7 is 10.43 kW·h, which saves 5.28 kW·h compared with 15.71 kW·h of the traditional scheme. The proportion reached 33.61%. However, the dispatched value of Experiment 4 is 12.04 kW·h at the maximum in the 10 simulations, saving 3.67 kW·h, and the energy-saving ratio is 23.36%. The average value of ten experiments is 11.24 kW·h, and the average energy saving ratio reaches 28.45%. It is not difficult to see that the energy-saving effect after optimization is more obvious.

TABLE 3. 5×15×2 scheduling scale energy consumption comparison

Experiment number	Dispatched value/kW·h	Average value/kW·h	Energy consumption value of traditional scheme/kW·h	Energy consumption difference/kW·h	Energy saving ratio
1	11.57			4.14	26.35%
2	10.93			4.78	30.43%
3	11.42			4.29	27.31%
4	12.04			3.67	23.36%
5	10.58	11.24	15.71	5.13	32.65%
6	11.22			4.49	28.58%
7	10.43			5.28	33.61%
8	10.82			4.89	31.13%
9	11.96			3.75	23.87%
10	11.46			4.25	27.05%

The scheduling gantt chart is shown in Figure 11. The overall scheduling process can be divided into two time periods, 0 to 2000 min and 3000 to 4000 min. There are no working cells in 2000 to 3000 min because all the current battery packs have been put on hold in the low-temperature discharge capacity test.

The detection channel scheduling sequence of Experiment 7 is shown in the table 4 (the sequence of working units has been arranged in the order of starting work). From the data in the table, it is clear that the scheduling scheme for the current optimal outcome is not unique. As in detection channel 2, O_{111} and O_{511} produce a new scheduling sequence after swapping the order of detection. However, since the current simulation experiment has the same battery pack information and the same detection task, the difference is only the inconsistency of the battery pack serial number. Therefore the new scheduling sequence is equivalent to the original scheduling sequence.
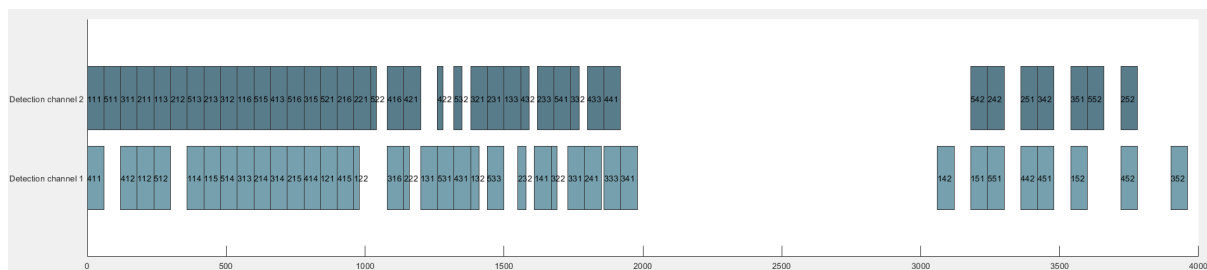
FIGURE 11. 5×15×2 scheduling gantt chart

4.2. 10×15×4 scheduling scale energy consumption simulation experiment. In this experiment, the batch of battery packs is 10, that is, the total number of test working units is 150, the number of detection channels is increased to 4, and the test scale can be expressed as 10×15×4 scheduling scale. The battery pack has a rated voltage of 25.6V and a rated capacity of 100Ah. The maximum delivery period is 240h. Simulation experiment 2 also takes 10 calculation results, and the energy consumption results retain two decimal places. The data are shown in Table 5.

TABLE 4. $5 \times 15 \times 2$ scheduling work sequence information

Channel information	Unit of work sequence
Detection channel 1	$O_{411}, O_{412}, O_{112}, O_{512}, O_{114}, O_{115}, O_{514}, O_{313}, O_{214}, O_{314},$ $O_{215}, O_{414}, O_{121}, O_{415}, O_{122}, O_{316}, O_{222}, O_{131}, O_{531}, O_{431},$ $O_{132}, O_{533}, O_{232}, O_{141}, O_{322}, O_{331}, O_{241}, O_{333}, O_{341}, O_{142},$ $O_{151}, O_{551}, O_{442}, O_{451}, O_{152}, O_{452}, O_{352}$
Detection channel 2	$O_{111}, O_{511}, O_{311}, O_{211}, O_{113}, O_{212}, O_{513}, O_{213}, O_{312}, O_{116},$ $O_{515}, O_{413}, O_{516}, O_{315}, O_{521}, O_{216}, O_{221}, O_{522}, O_{416}, O_{421},$ $O_{422}, O_{532}, O_{321}, O_{231}, O_{133}, O_{432}, O_{233}, O_{541}, O_{332}, O_{433},$ $O_{441}, O_{542}, O_{242}, O_{251}, O_{342}, O_{351}, O_{552}, O_{252}$

TABLE 5. $10 \times 15 \times 4$ scheduling scale energy consumption comparison

Experiment number	Dispatched value/kW·h	Average value/kW·h	Energy consumption value of traditional scheme/kW·h	Energy consumption difference/kW·h	Energy saving ratio
1	21.57			9.67	30.78%
2	20.98			10.44	34.31%
3	20.63			11.06	35.20%
4	21.54			9.88	31.44%
5	21.43	20.89	31.42	9.99	31.79%
6	19.87			11.55	36.76%
7	20.31			11.11	35.60%
8	20.12			11.30	35.96%
9	21.56			9.86	31.38%
10	20.71			10.71	34.09%

It can be seen from the data in Table 5 that the dispatching effect of Experiment 6 is the best among the current ten experiments, and its dispatched value is 19.87 kW·h, which is 11.55 kW·h less than the traditional scheme, and the energy saving ratio reaches 36.76%. The dispatch value of 21.75 kW·h in Experiment 1 is the largest among the ten experiments, and its energy-saving ratio has reached 30.78%. In Experiment 2, the dispatching average of ten experiments is 20.89 kW·h, and the average energy-saving ratio reaches 33.51%, which is slightly higher than the average energy-saving ratio in Experiment 1. The main reason for this phenomenon is that the efficiency of the equipment feeding back the power grid is lower than that of feeding back the DC/DC module. With the increase of the dispatch scale and the increase of the detection channel, the energy flow mode between the battery packs increases during the test, resulting in The losses are lower than those incurred when feeding energy back to the grid.

The scheduling gantt chart of Experiment 6 is shown in Figure 12. The overall process is also divided into two periods, from 0 to 2500 min and from 2600 to 4200 min. From the electrical performance test task information, it is known that the low-temperature discharge capacity test specifies that the battery's shelving time is 1500 min. When the batteries are all in this state, a longer shelving phase will be generated. The detection channel sequence information is shown in Table 6. Where the work units in the channel

have been prioritized in order of start time. The optimal solution corresponding to the scheduling scheme is again not unique.
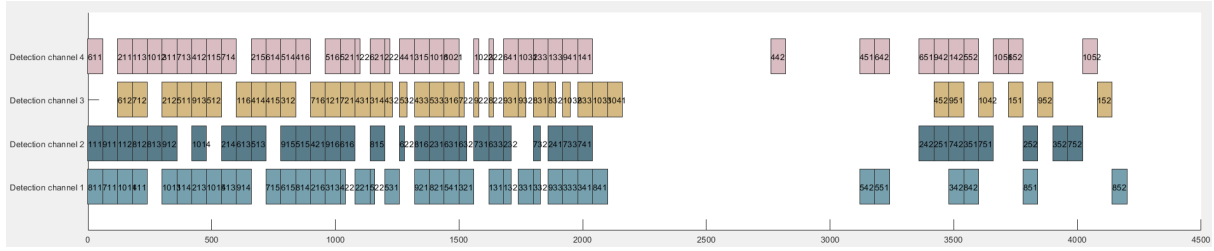
FIGURE 12. 10×15×4 scheduling gantt chart

TABLE 6. 10×15×4 scheduling work sequence information

Channel information	Unit of work sequence
Detection channel 1	O_{811}, O_{711}, O_{1011}, O_{411}, O_{1013}, O_{114}, O_{213}, O_{1015}, O_{413}, O_{914}, O_{715}, O_{615}, O_{814}, O_{216}, O_{313}, O_{422}, O_{221}, O_{522}, O_{531}, O_{921}, O_{821}, O_{541}, O_{321}, O_{131}, O_{132}, O_{331}, O_{332}, O_{933}, O_{333}, O_{341}, O_{841}, O_{542}, O_{551}, O_{342}, O_{842}, O_{851}, O_{852}
Detection channel 2	O_{111}, O_{911}, O_{112}, O_{812}, O_{813}, O_{912}, O_{1014}, O_{214}, O_{613}, O_{513}, O_{915}, O_{515}, O_{421}, O_{916}, O_{616}, O_{815}, O_{622}, O_{816}, O_{231}, O_{631}, O_{632}, O_{731}, O_{633}, O_{232}, O_{732}, O_{241}, O_{733}, O_{741}, O_{242}, O_{251}, O_{742}, O_{351}, O_{751}, O_{252}, O_{352}, O_{752}
Detection channel 3	O_{612}, O_{712}, O_{212}, O_{511}, O_{913}, O_{512}, O_{116}, O_{414}, O_{415}, O_{312}, O_{716}, O_{121}, O_{721}, O_{431}, O_{314}, O_{432}, O_{532}, O_{433}, O_{533}, O_{316}, O_{722}, O_{922}, O_{822}, O_{931}, O_{932}, O_{831}, O_{832}, O_{1032}, O_{833}, O_{1033}, O_{1041}, O_{452}, O_{951}, O_{1042}, O_{151}, O_{952}, O_{152}
Detection channel 4	O_{611}, O_{211}, O_{113}, O_{1012}, O_{311}, O_{713}, O_{412}, O_{115}, O_{714}, O_{215}, O_{614}, O_{514}, O_{416}, O_{516}, O_{521}, O_{122}, O_{621}, O_{222}, O_{441}, O_{315}, O_{1016}, O_{1021}, O_{1022}, O_{322}, O_{641}, O_{1031}, O_{233}, O_{133}, O_{941}, O_{141}, O_{442}, O_{451}, O_{642}, O_{651}, O_{942}, O_{142}, O_{552}, O_{1051}, O_{652}, O_{1052}

5. **Conclusions.** In this paper, the scheduling target with the lowest power consumption of test equipment is the optimization object, and a multi-machine scheduling model based on the scheduling target is established. Four specific modes of energy flow in the entire detection process are deduced in detail, which provides a theoretical basis and solution method for calculating the value of the objective function. Through a two-layer coding method, the mapping relationship between population individuals and scheduling schemes is successfully established. A calculation rule for the start time of the work unit test in the scheduling sequence is proposed, and the start time is arranged for the scheduling sequence generated by each test channel, so that the generated scheduling scheme is perfected.And the optimal scheduling scheme is successfully solved by PSO. Finally, through simulation experiments, the method proposed in this paper can reduce the energy consumption of testing equipment by 30% compared with traditional methods, and successfully improves the energy saving performance of testing equipment.

REFERENCES

[1] W.-J. Fu, X.-Y. Wang, W. Ke, and C.-F. Ding, "An Important Development Direction for Vehicle Electrification - Lithium Battery Technology," *New Energy Automobile*, vol. 07, no. 403, pp. 123-125, 2023.

[2] C.-B. Liu, and F. Wang, "State Detection System of Electric Vehicle Battery Pack," *Instrument Technique and Sensor*, vol. 10, no. 477, pp. 123-126, 2022.

[3] Ministry of Industry and Information Technology of the People's Republic of China, "Electrical Performance Requirements and Test Methods for Traction Batteries for Electric Vehicles," GB/T 31486-2015, 2015.

[4] Z. Li, and S.-N. Zhou, "High Dimensional Multi-objective Dynamic Job Shop Scheduling Optimization for Green Intelligent Manufacturing," *Operations Research and Management Science*, vol. 32, no. 1, pp. 47-53, 2023.

[5] J.-C. Gu, T.-H. Jiang, and H.-Q. Zhu, "Energy-saving Job Shop Scheduling Problem with Multi-objective Discrete Grey Wolf Optimization Algorithm," *Computer Integrated Manufacturing Systems*, vol. 27, no. 8, pp. 2295-2306, 2021.

[6] T.-H. Jiang, "Low-carbon Workshop Scheduling Problem Based on Grey Wolf Optimization," *Computer Integrated Manufacturing Systems*, vol. 24, no. 10, pp. 2428-2435, 2018.

[7] H.-T. Tang, and Y. Zhang, "A Research on Hybrid Flow Shop Scheduling Based on Green Production," *Industrial Engineering Journal*, vol. 25, no. 3, pp. 115-123, 2022.

[8] L. Fang, W.-X. Ji, W. Peng, and C. Feng, "Optimal Scheduling of Storage Energy Consumption Under Dynamic Storage Allocation Strategy," *Computer Engineering and Applications*, vol. 2, no. 2, pp. 303-311, 2023.

[9] J. Xue and B. Shen, "Novel Imperialist Competitive Algorithm for Many-objective Flexible Job Shop Scheduling," *Control Theory & Applications*, vol. 36, no. 6, pp. 893-901, 2019.

[10] G. Wang, S. Gao, and S. Fang, "Multi-objective Flexible Job-shop Scheduling Based on Adaptive NSGA-II," *Machine Tool & Hydraulics*, vol. 50, no. 18, pp. 129-135, 2022.

[11] D. Fang, Z.-G. Jiang, and W. Yan, "A Lot Splitting Scheduling Method for Green Workshop Based on Multi-level Optimization Model," *Manufacturing Automation*, vol. 45, no. 3, pp. 81-86+98, 2023.

[12] X.-L. Wu, and Y.-J. Sun, "A Green Scheduling Algorithm for Flexible Job Shop with Energy-saving Measures," *Journal of Cleaner Production*, vol. 172, pp. 3249-3264, 2018.

[13] A. Amirteimoori, E.-B. Tirkolaee, V. Simic, and G.-W. Weber, " A parallel heuristic for hybrid job shop scheduling problem considering conflict-free AGV routing," *Swarm and Evolutionary Computation*, vol. 79, pp. 101312, 2023.

[14] J.-X. Shi, M.-Z. Chen, Y.-M. Ma, and F. Qiao, "A New Boredom-Aware Dual-Resource Constrained Flexible Job Shop Scheduling Problem Using a Two-Stage Multi-Objective Particle Swarm Optimization Algorithm," *Information Sciences*, vol. 643, pp. 119141, 2023.

[15] Z.-Q. Tian ,X.-Y. Jiang ,W.-J. Liu, and Z.-W. Li, "Dynamic Energy-efficient Scheduling of Multi-variety and Small Batch Flexible Job-shop: A Case Study for the Aerospace Industry," *Computers & Industrial Engineering*, vol. 178, pp. 109111, 2023.

[16] H.-L. Liu , J.-H. Zhang , and T. Xie, "Job Shop Scheduling Problem (JSP) Research Review Report," *Equipment Manufacturing Technology*, vol. 12, pp. 235-237, 2015.

[17] J.-P. Guo, G.-B. Zhong, K.-Q. Xu , W. Su, and H.-F. Xiang, " The Characteristics of LiFePO4 Batteries by Comparison Constant Power Test with Constant Current Test," *Chinese LABAT Man*, vol. 54, no. 3, pp. 109-115, 2017.

[18] H. Lu, X. Li, and R.-L. Lang, *Theory and Method of Automatic Test Task Scheduling Problem*, National Defense Industry Press, Beijing, 2014.

[19] S.-Z. Yu, "Research on Battery Life Prediction Method of Electric Vehicle Based on Real-time Data, " Ph.D. dissertation, Harbin Institute of Technology, 2021.

[20] T.-Y. Wu, A.-K. Shao, and J.-S. Pan, "CTOA: Toward a Chaotic-Based Tumbleweed Optimization Algorithm, Mathematics, " *Mathematics*, vol. 11, no. 10, pp. 2339, 2023.

[21] T.-Y. Wu, H.-N. Li, and S.-C. Chu, "CPPE: An Improved Phasmatodea Population Evolution Algorithm with Chaotic Maps, " *Mathematics*, vol. 11, no. 9, pp. 1977, 2023.

[22] J. Kennedy and R. Eberhart, "Particle Swarm Optimization," in *Proceedings of ICNN'95 - International Conference on Neural Networks*. IEEE, 1995, vol. 4, pp. 1942-1948.

[23] M.-N. Xu, and B. Chen, "Research on Job Shop Scheduling Optimization Based on Improved Cuckoo Search Algorithm," *Journal of Chinese Computer Systems*, vol. 42, no. 9, pp. 1826-1829, 2021.